Anesthesiology
V 45, No 2, Aug 1976

Hemodynamic Monitoring:

Noninvasive Techniques

Laura F. Wexler, M.D., and Gerald M. Pohost, M.D.†*

TECHNIQUES IN CARDIOLOGY that do not involve placement of a catheter into a cardiac chamber or great vessel are called "noninvasive." They have been used largely for diagnostic purposes, but offer an enormous potential for future evaluation of physiologic performance during acute perturbations induced by anesthetics, operations and acute illness. The "noninvasive" techniques include, among others, electrocardiography, vectorcardiography, and phonocardiography, all of which have been used for several decades; echocardiography and radionuclide imaging techniques, developed in the past decade, will require further innovative engineering to allow for routine monitoring of the critically ill. Table 1 lists the noninvasive techniques presently available. The following discussion deals mainly with the newer noninvasive methods that have potential application to perioperative evaluation and monitoring. These include echocardiography, systolic time intervals, and radionuclide imaging techniques.

Echocardiography

BASIC PRINCIPLES

When a beam of high-frequency sound, or ultrasound, encounters an interface between two media of different densities, part of the beam will be reflected and the remainder transmitted. Echocardiography is defined as the analysis of ultrasound reflected from cardiac structures.

Diagnostic ultrasound, which has a frequency of 1 to 10 million cycles per second, is generated by a piezoelectric crystal. This crystal vibrates under the influence of an electric field and emits ultrasound. Conversely, when ultrasound interacts with the same piezoelectric crystal, electrical signals are produced.

An ultrasound transducer consists of a piezoelectric crystal located in a cylindrical probe and a lens in front of the crystal. The crystal is electrically stimulated to emit ultrasound, which is collimated, or focused, into a beam by the lens. The beam is directed at the heart through the chest wall. Ultrasound reflected from the cardiac structures is received by the transducer and interacts with the crystal to produce electrical signals, which are amplified and displayed on a cathode-ray tube. The transducer acts as both transmitter and receiver. The entire system is called an echograph.

The speed of sound within the heart and surrounding structures is assumed to be constant, and thus the distance between any reflecting structure and the transducer surface can be derived from the interval between transmission and reception of reflected ultrasound. Circuitry within the echograph allows display of the transducer surface as well as position of reflecting structures by converting time interval between transmission and reception of ultrasound impulses into actual distance. A strip-chart recorder continuously records the oscilloscopic image obtained with the echograph so that motion as well as position of the reflecting structures can be assessed. Echocardiographic examination permits a beat-by-beat observation of the position, motion, and relative intensity of reflected ultrasound from the valves and the ventricular walls.

Ultrasound is poorly transmitted through lung and bone. Regions of the anterior chest wall through which the ultrasound beam is most successfully transmitted are called "windows." These "windows" are located along the left sternal border and the lower left chest toward the cardiac apex. Occa-

* Clinical and Research Fellow in Medicine.
† Instructor in Medicine.
Received from the Cardiac Unit at the Massachusetts General Hospital, Boston, Massachusetts.
Address reprint requests to: Laura F. Wexler, M.D., Cardiac Unit, Massachusetts General Hospital, Boston, Massachusetts 02114.

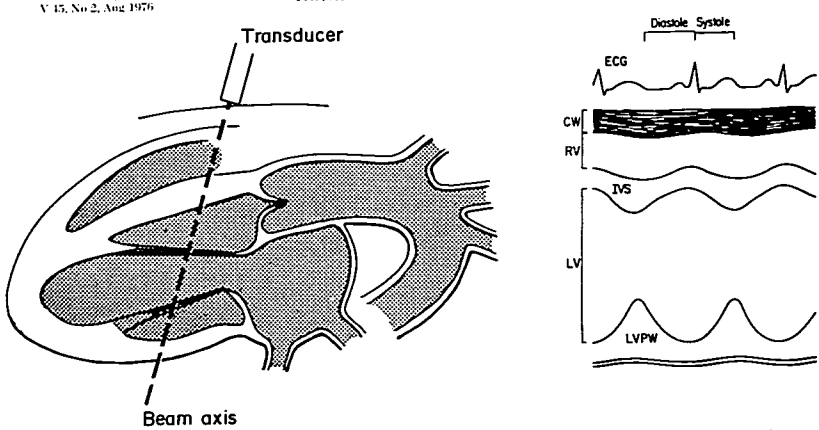

FIG. 1. The diagram on the left depicts a sagittal section through the heart with the apex on the left and base and aorta on the right. The ultrasound beam is aimed to traverse the ventricular chambers and interventricular septum. The diagram on the right depicts the echocardiogram obtained from this transducer position. ECG = electrocardiogram, CW = chest wall, RV = right ventricle, IVS = interventricular septum, LV = left ventricle, and LVPW = left ventricular posterior wall.

TABLE 1. Noninvasive Techniques

Technique	Description
Phonocardiography	Analysis of graphic recordings of sounds emanating from the heart and great vessels
Apexcardiography	Study of recordings of precordial impulses relative to the chest wall
Kinetocardiography	Study of recordings of multiple precordial impulses relative to a fixed external point
Ballistocardiography	Analysis of graphic recordings of the movement of the body caused by cardiac contraction and acceleration or deceleration of blood within the great vessels
Radarkymography	Analysis of cardiac border movement by videotracking of roentgenographic images
Systolic and diastolic time intervals	Analysis of time intervals derived from the electrocardiogram, phonocardiogram, carotid pulse-wave recording and apexcardiogram
Doppler ultrasonography	Use of shifts in frequency of reflected ultrasound to determine velocity of blood flow through cardiac chambers and great vessels
Echocardiography	Use of reflected ultrasound to study location and motion of cardiac structures
Radionuclide imaging technique	Use of radionuclides, *i.e.*, radioactive tracers, to visualize cardiac chambers, myocardium and myocardial infarct

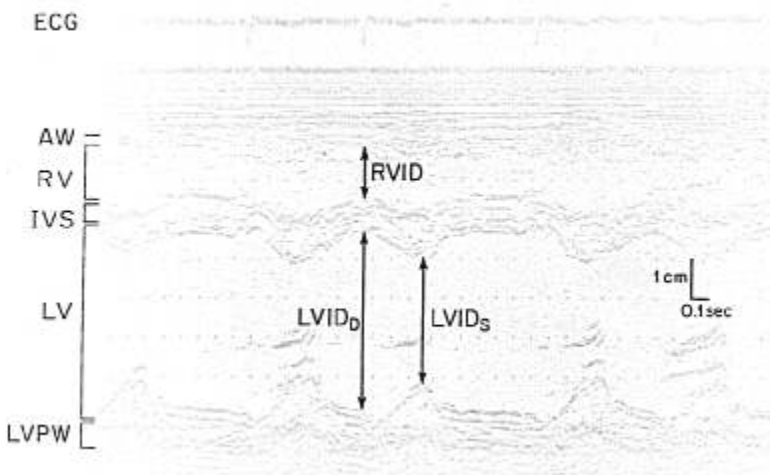

FIG. 2. Echocardiogram showing the right ventricle (RV), interventricular septum (IVS), and left ventricle (LV). ECG = electrocardiogram, AW = right ventricular anterior wall, LVPW = left ventricular posterior wall, RVID = right ventricular internal dimension measured at end-diastole. $LVID_D$ = left ventricular internal dimension measured at end-diastole (indicated by peak of QRS complex), $LVID_S$ = left ventricular internal dimension measured at end-systole (indicated by end of T-wave on ECG).

On the strip-chart recording above, time and distance are indicated by markers (dots) that are 1 cm apart in the vertical axis and 0.2 seconds apart in the horizontal axis.

sionally, to obtain an adequate window, a subxyphoid or suprasternal notch approach can be employed.

Examination of the Left Ventricle and Interventricular Septum

Figure 1 depicts the ultrasound beam as it traverses the ventricles and the interventricular septum. The resultant echocardiogram is illustrated in figure 2. After the chest wall, the beam encounters the right ventricular free wall. During systole it moves posteriorly away from the transducer toward the interventricular septum. The cavity of the right ventricle is filled with blood of homogeneous acoustic density and thus is "echo-free." The next structure encountered is the interventricular septum. The normal interventricular septum moves posteriorly in systole and anteriorly in diastole. The left ventricular posterior wall moves anteriorly towards the septum during systole. Both septum and posterior wall normally thicken during systole. The motion and thickness of the left ventricular walls, both free wall and interventricular septum, and left ventricular chamber size can be assessed from this echocardiographic axis. Noninvasive assessment of left ventricular size and function is one of the most important applications of echocardiography. Although used principally for diagnostic purposes, the quality of information obtained to date suggests that an extension to the intraoperative monitoring of ventricular function may be possible.

A measurement of the thickness of the interventricular septum and left ventricular posterior wall can be made, as indicated in figure 2. These measurements have been shown to correlate with measurements made

during cardiac surgery and postmortem examination.[1,2] Normally, the interventricular septum and the left ventricular posterior wall are of comparable thicknesses (less than 1.2 cm). Concentric left ventricular hypertrophy, secondary to aortic stenosis or arterial hypertension, can be demonstrated on echo as symmetric thickening of interventricular septum and left ventricular posterior wall. Asymmetric thickening of the interventricular septum compared with the left ventricular posterior wall (in a ratio of 1.3 to 1.0 or greater) is a feature of hypertrophic cardiomyopathy and can be documented by echocardiogram, as shown in figure 3.[3]

Internal dimension of the left ventricle can be measured in both end-systole and end-diastole (see figures 1 and 2). When made in a standard fashion such that the beam transects the left ventricular cavity at a level immediately below the mitral valve leaflets, echocardiographic internal dimensions correlate well with left ventricular dimensions determined angiographically.[4] The ejection fraction‡ can be approximated from these echocardiographic dimensions.[5] The technique is

‡ The ejection fraction, EF, is the ratio of left ventricular stroke volume to end-diastolic volume. $EF = \frac{EDV - ESV}{EDV}$ where EDV = end-diastolic volume and ESV = end-systolic volume. The normal value determined angiographically is 60–75%. A decrease in ejection fraction secondary to either reduction in stroke volume or increase in end-diastolic volume without concomitant increase in stroke volume is a reliable indicator of left ventricular failure.

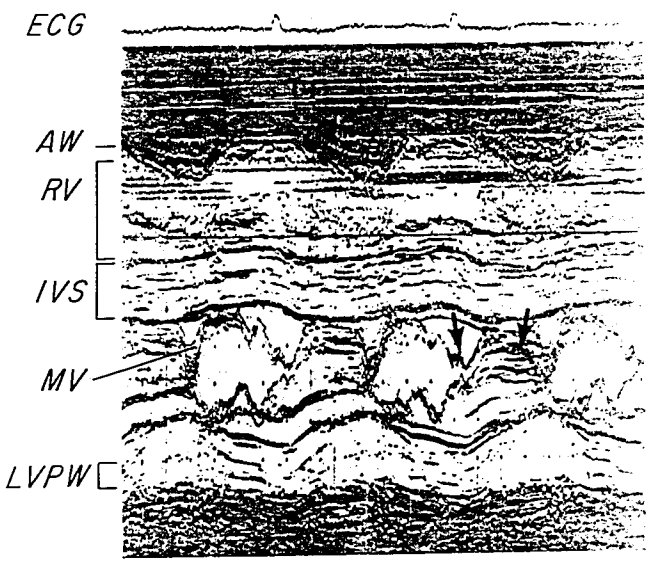

FIG. 3. Echocardiogram of the interventricular septum, mitral valve, and left ventricular posterior wall from a patient with idiopathic hypertrophic subaortic stenosis. Characteristic abnormalities demonstrated include 1) asymmetric septal hypertrophy (ASH) with an interventricular septal (IVS) thickness of 1.4 cm and a posterior wall (LVPW) thickness of 0.8 cm, 2) systolic anterior motion of the anterior mitral valve leaflet (MV) indicated by the arrow on right, 3) delayed mitral valve closure with a "shoulder" indicated by arrow on left. This finding is associated with elevated left ventricular end-diastolic pressure. 4) Reduced E to F slope of the mitral valve (see text and figure 6*B*). AW = right ventricular anterior wall, RV = right ventricular cavity.

limited since it uses a single dimension to derive end-diastolic and end-systolic volumes. This limitation is especially important in patients with ischemic heart disease, who frequently have regional wall motion abnormalities.[6,7] However, the technique may be of great value when one is following performance in the course of physiologic perturbations, particularly if one looks for changes rather than absolute values. Another index of left ventricular contractility, the circumferential fiber shortening velocity, can be derived from end-systolic and end-diastolic dimensions.[8]

An increase in left ventricular end-diastolic dimension is seen in congestive cardiomyopathy, and/or left ventricular volume overload secondary to mitral and aortic regurgitation or ventricular septal defect. In congestive cardiomyopathy, amplitude of left ventricular wall motion is attenuated, while in left ventricular volume overload, wall motion may be accentuated. Decreased or absent motion of the interventricular septum and/or left ventricular posterior wall may also be detected in a patient with myocardial infarction.[9]

Right Ventricle (RV)

The internal dimension of the RV can be determined echocardiographically as shown in figure 2. It may be increased in association with a number of clinical states, including right ventricular volume overload (atrial septal defect, tricuspid regurgitation), congestive cardiomyopathy, and right ventricular failure. Another indication of RV volume overload is paradoxic motion of the interventricular septum.[10] Normally, the septum

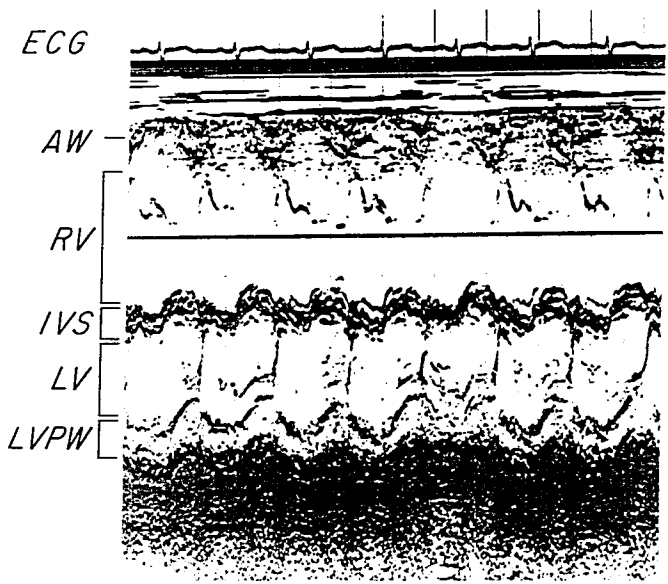

FIG. 4. Echocardiogram of right ventricle (RV), left ventricle (LV), and interventricular septum (IVS) from a patient with an atrial septal defect. The right ventricle is enlarged and the interventricular septum moves paradoxically away from the left ventricular posterior wall during systole. AW = right ventricular anterior wall, LVPW = left ventricular posterior wall.

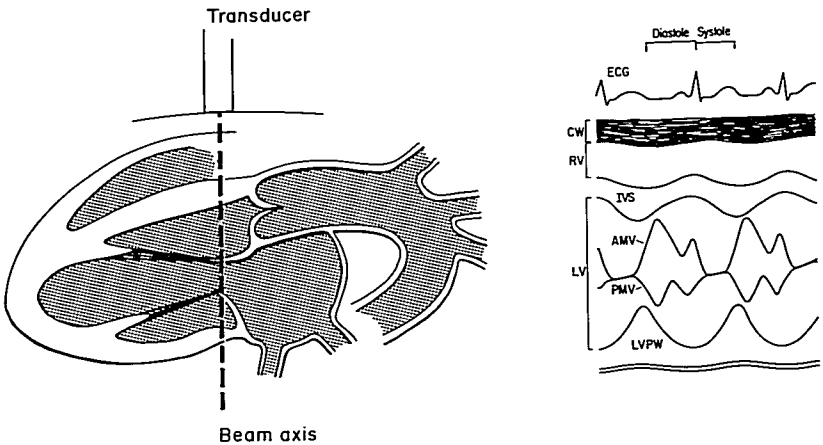

FIG. 5. Sagittal view of the heart, on the left, demonstrates the ultrasound beam traversing the chest wall (CW), anterior wall, right ventricle (RV), interventricular septum (IVS), left ventricle (LV), anterior leaflet of the mitral valve (AMV), posterior leaflet of the mitral valve (PMV), and the left ventricular posterior wall (LVPW). On the right is a diagram of the strip-chart recording of the resulting echocardiogram. The structures in the diagram of the heart on the left are matched with the echocardiogram on the right.

moves toward the left ventricular posterior wall during systole. Figure 4 shows an example of paradoxic motion of the septum away from the left ventricular posterior wall during systole in a patient with an atrial septal defect. Paradoxic septal motion can also be seen in patients with ventricular conduction defects and following cardiopulmonary bypass; it is not clear whether this finding is entirely specific for abnormal increase in RV volume.

MITRAL VALVE

Figure 5 shows the image obtained with the ultrasound beam aimed at the mitral valve leaflets. Normally, the anterior leaflet of the mitral valve has a distinctive "M"-shaped configuration in diastole (fig. 6, *A* and *B*). In early diastole, the anterior leaflet moves anteriorly towards the chest wall, while the posterior leaflet moves in the opposite direction. The point of maximum early diastolic excursion is designated E. After the E point, the leaflets drift towards each other to point F in mid-diastole. With atrial systole, the leaflets again separate widely to point A and then move rapidly towards each other as the valve closes, C. During ventricular systole, the closed leaflets move slowly anteriorly to the D point immediately prior to diastolic separation. This motion may be related to forward motion of the mitral annulus during systole.

Changes in the slope of early diastolic motion of the anterior mitral valve leaflet, the "E-to-F slope," can be an important clue to abnormalities in left ventricular and mitral valve function. The E-to-F slope appears to be related to the rate of diastolic filling of the left ventricle. A decreased E-to-F slope may be observed in patients with diminished left ventricular compliance associated with hypertrophic or congestive cardiomyopathy.[11] The E-to-F slope is also diminished in patients with mitral stenosis, and the extent of flattening correlates with the severity of stenosis as estimated at operation or calculated by the Gorlin formula at the time of cardiac cathe-

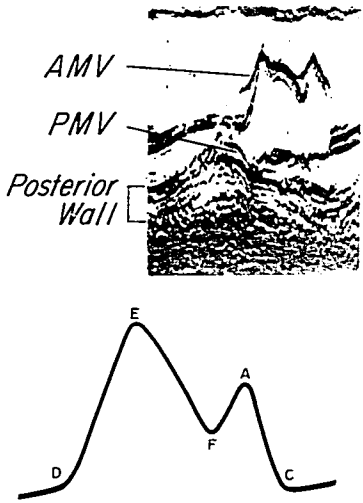

FIG. 6. *A* (*above*), representative echocardiogram of a normal mitral valve. AMV = anterior mitral valve leaflet. PMV = posterior mitral valve leaflet. Mitral valve motion during diastole results in a characteristic "M"-shaped configuration (see text). *B* (*below*), diagram of motion of the anterior mitral valve leaflet as recorded by echocardiogram. At point D, the anterior leaflet moves rapidly anteriorly in early diastole. E is the point of maximum early diastolic excursion. At point F, the leaflet drifts posteriorly in mid-diastole approaching the posterior leaflet (not illustrated). The leaflet again moves rapidly anteriorly in late diastole as the atrium contracts to point A. With the onset of ventricular systole, the leaflet moves rapidly posteriorly to the closed position at point C.

terization.[12] Patients with abnormal E-to-F slopes secondary to mitral stenosis can usually be differentiated from those with left ventricular dysfunction by the presence of abnormal parallel motion of the posterior leaflet (fig. 7), a finding more specific for mitral stenosis.[13]

No characteristic abnormality of mitral valve motion is observed in patients with rheumatic regurgitation of papillary muscle dysfunction. Indirect evidence, such as left ventricular and/or left atrial enlargement and increased left ventricular wall excursion, is frequently present. Certain abnormalities of the mitral valve known to be associated with mitral regurgitation can be diagnosed or suggested by echocardiogram. Mitral valve prolapse is a condition in which one or both leaflets move back into the left atrium during systole. Abnormal posterior motion of one or both leaflets, usually during mid or late systole, is frequently observed on echocardiogram in patients with mitral valve prolapse[14,15] (fig. 8). Prolapse may be seen in patients with or without mitral regurgitation but is frequently associated with the characteristic mid-systolic click and late systolic murmur. Flail mitral valve leaflets secondary to ruptured chordae tendineae or papillary muscle can also be suggested by echocardiogram.

The echocardiogram of the anterior leaflet of the mitral valve characteristically shows abnormal anterior systolic motion in patients with idiopathic hypertrophic subaortic stenosis (IHSS).[16] In addition to abnormal anterior systolic motion of the mitral valve, asymmetric hypertrophy of the interventricular septum is also characteristic of IHSS (fig. 3). The abnormal systolic position of the mitral valve and the asymmetric hypertrophy of the interventricular septum result in the mitral regurgitation and outflow gradient often present in this disease.[17]

Premature closure of the mitral valve is observed in patients with acute, severe aortic regurgitation, which is most commonly associated with bacterial endocarditis[18] and may help in identification of patients requiring valve replacement. In many patients, the presence of aortic regurgitation of even moderate degree can be detected by fine fluttering of the anterior mitral valve leaflet during diastole, presumably related to motion of the leaflet within the regurgitant stream.

Abnormal left ventricular function may also be suggested by altered morphology of mitral valve closure during the A-to-C interval (see fig. 6*B*). In some patients with marked elevation of left ventricular end-diastolic pressure, the normally rapid and smooth posterior closure motion of the anterior mitral valve leaflet is interrupted by the appearance of a "shoulder" and the A-to-C interval may be prolonged[19] (see fig. 3).

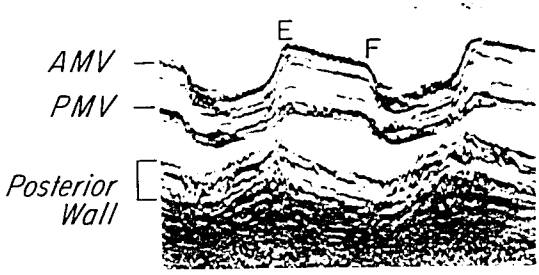

FIG. 7. Echocardiogram of the mitral valve from a patient with mitral stenosis. The E-to-F slope of the anterior mitral valve leaflet (AMV) is diminished and the motion of the posterior mitral valve leaflet (PMV) in diastole is parallel to that of the AMV.

AORTA AND LEFT ATRIUM

When the transducer is angled superiorly and slightly medially, the ultrasound beam will traverse the aortic root and the left atrium (fig. 9A). Aortic root and left atrial dimensions measured from the echocardiogram correlate well with aortic root diameter and left atrial size determined angiographically.[20] As a rule of thumb, the normal aortic root dimension measured at end-diastole is approximately equal to the left atrial dimension measured at end-systole. Thus, any significant disproportionate increase in either aortic root or left atrial echocardiographic dimension represents abnormal enlargement.[21] Figure 10 shows the echocardiogram of a patient with left atrial enlargement due to mitral stenosis.

Left atrial myxomas have a characteristic echocardiographic pattern.[22] These tumors are usually on a stalk originating in the left

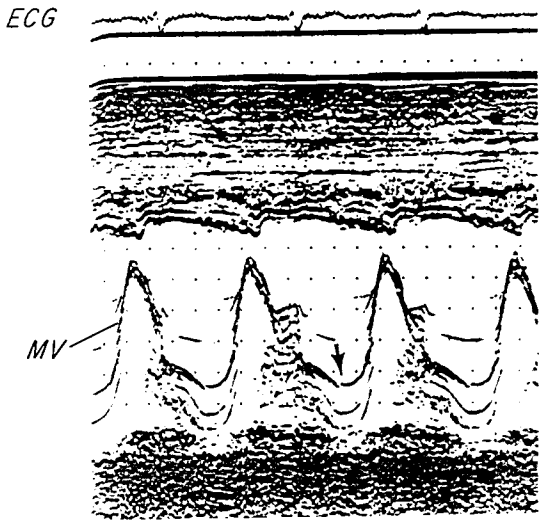

FIG. 8. Echocardiogram of a patient with mitral valve prolapse. During systole the mitral valve leaflets sag or prolapse posteriorly (see arrow). ECG = electrocardiogram, MV = mitral valve.

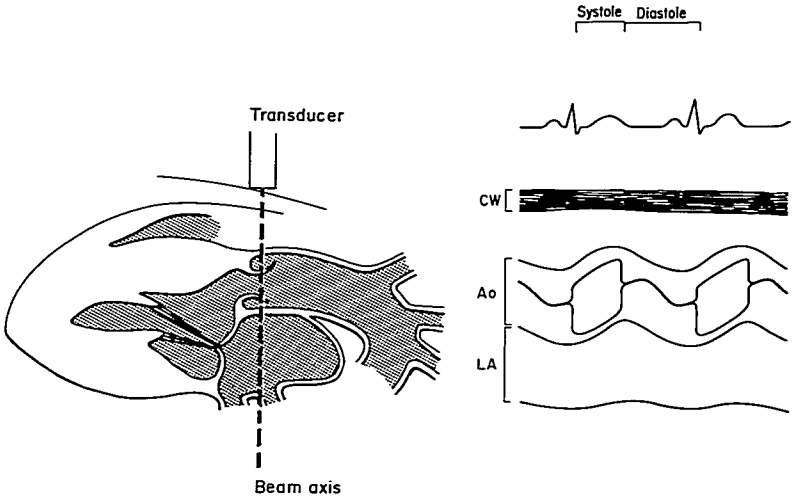

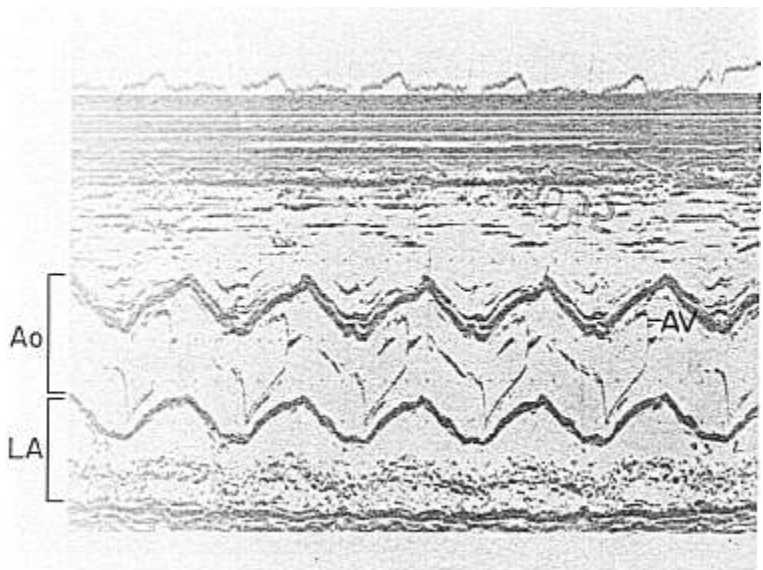

FIG. 9. *A* (*above*), sagittal view of the heart, on the left, demonstrates the ultrasound beam traversing the aorta (Ao) at the level of the aortic valve leaflets, and the left atrium (LA). Diagram on the right depicts resultant echocardiogram. CW = chest wall. *B* (*below*), echocardiogram of the aorta (Ao), left atrium (LA) and aortic valve (AV). The characteristic parallelogram pattern of the aortic leaflets is demonstrated.

atrium and prolapse into the left ventricle in diastole. On echocardiogram, dense echos are observed within the left atrium and in the area of the mitral valve in diastole (see fig. 11). Left atrial clot cannot reliably be detected by echocardiogram at this time.

The motion of the aortic valve produces a box-like configuration on echocardiogram (fig. 9*B*) that reflects abrupt leaflet separation at onset of left ventricular systole and rapid closure at end-systole (fig. 9*B*).

Calcification or thickening of the aortic valve is suggested by dense echos between the aortic walls (fig. 12), but unfortunately the severity of aortic stenosis cannot be assessed reliably by echocardiography.[23] The echocardiogram of the aortic valve does not reliably depict orifice size. Young patients with congenital aortic stenosis frequently have a domed aortic valve with normal leaflet separation at the base during ejection. Thus, if the echo beam traverses the aortic valve near its base, a normal configuration may be observed. Patients with calcified aortic valves but without significant stenosis may have dense aortic valve echos with reduced separation. Two-dimensional echocardiography, presently under investigation, may be able

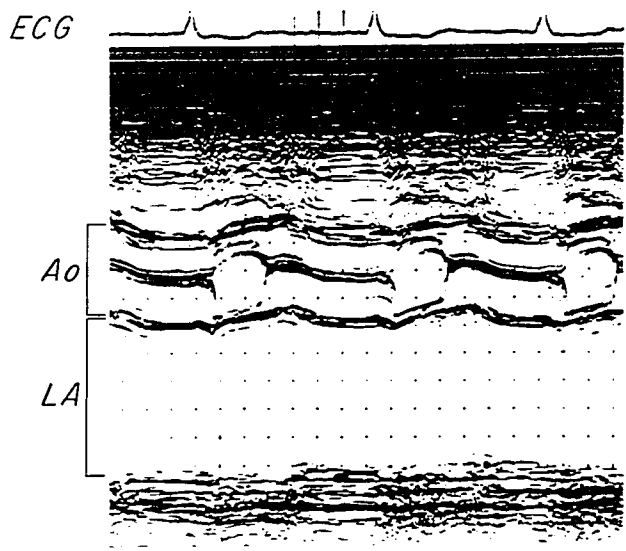

FIG. 10. Echocardiogram from a patient with mitral stenosis showing the aorta (Ao), which is 3.2 cm. in diameter, and the disproportionately enlarged left atrium (LA), which measures 5.5 cm. The aortic valve leaflets move normally.

FIG. 11. Echocardiographic "scan" from the level of the anterior leaflet of the mitral valve and interventricular septum (IVS) (*left*) to the level of the aorta (Ao) and left atrium (LA) (*right*) in a patient with a left atrial myxoma. The myxoma shows a cloud of echos behind the anterior leaflet of the mitral valve in diastole and a cloud of echos within the left atrium in systole. RV = right ventricle.

more reliably to assess aortic valve area in aortic stenosis.[24]

TRICUSPID VALVE

The tricuspid valve can be imaged by tilting the transducer inferiorly to the aortic valve. The echocardiographic patterns of normal tricuspid valve motion, tricuspid stenosis, tricuspid valve prolapse and flail tricuspid valve leaflet resemble those of the similar processes involving the mitral valve.

PULMONIC VALVE

The pulmonic valve echocardiogram is to the left and slightly superior to the aortic valve but is often difficult to obtain in adults; usually only a single posterior leaflet can be defined. In late diastole, there is a transient posterior motion just before systolic opening that correlates with atrial systole and is called the pulmonic "a" wave (fig. 13). Pulmonary hypertension or pulmonic stenosis is suggested by changes in the normal echocardiographic pattern of the posterior leaflet of the pulmonic valve.[25,26] With pulmonary hypertension, the pulmonic "a" wave diminishes in depth and may disappear. In pulmonic stenosis, the "a" wave becomes deeper and the leaflet fails to return to baseline before systolic opening.

PERICARDIAL EFFUSIONS

In most patients, the epicardium and parietal pericardium appear as a single interface on the echocardiogram. When pericardial fluid is present, the epicardium is separated from the pericardium and an echo-free space can be detected (fig. 14). The depth of the echo-free space correlates grossly with the size of the effusion and can be used to detect increase or decrease in the size of the pericardial effusion.[27] There is no reliable way to make the diagnosis of pericardial tamponade on echocardiogram.

CONGENITAL HEART DISEASE

The echocardiogram can be helpful in the diagnostic assessment of patients with con-

genital heart disease. A complete review of echocardiography in congenital heart disease is beyond the scope of this monograph, and several comprehensive reviews are presently available. It is worth mentioning a few of the important applications. Right ventricular dilatation and paradoxic septal motion are associated with right ventricular volume overload states (*e.g.*, atrial septal defect). The tricuspid valve echocardiographic pattern is distinctive in patients with Ebstein's anomaly. Echocardiography is also helpful in identification of a hypoplastic right or left ventricle. An echocardiographic "scan" is obtained when the transducer is directed from one area of the heart (*e.g.*, aortic valve) to another (*e.g.*, mitral valve) while continuously recording on the strip chart. Echo "scans" are of value in the analysis of relationships between cardiac chambers and great vessels in the following lesions: transposition of the great arteries, truncus arteriosus, and tetralogy of Fallot. Many new applications of echocardiography to congenital heart disease have been described in the recent literature.[28] There is great potential in combining standard radiologic and radionuclide techniques with echocardiography to evaluate complex congenital lesions noninvasively.[29] The sector scanner, an ultrasound device, provides a two-dimensional image of the heart and appears to improve the diagnostic efficacy of echocardiography in congenital heart disease.

Summary

Echocardiography is a relatively new noninvasive technique that has proven itself in numerous clinical applications. It has, to some extent, replaced cardiac catheterization in the diagnosis of hypertrophic cardiomyopathy, left atrial myxoma, mitral stenosis, and mitral valve prolapse, and has allowed for a better patient evaluation prior to cardiac catheterization, which results in a better organized and thus shorter catheter study. Furthermore, it allows for noninvasive serial follow-up studies to evaluate the timing and need for as well as the results of operation. Two-dimensional echocardiography, or sector scanning, may

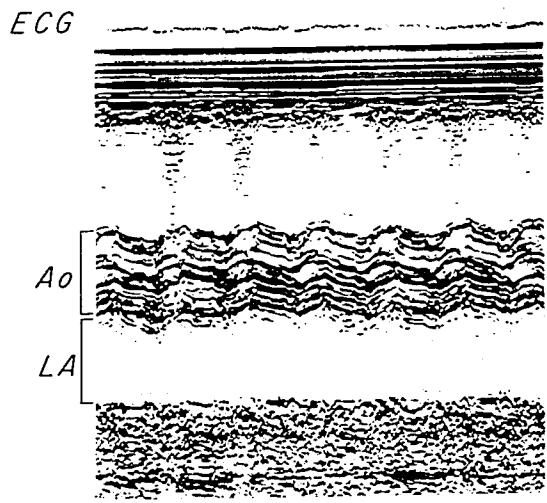

FIG. 12. Echocardiogram of the aortic valve of a patient with calcific aortic stenosis. Ao = aorta, LA = left atrium, ECG = electrocardiogram. Multiple dense echos in the region of the aortic valve are characteristic.

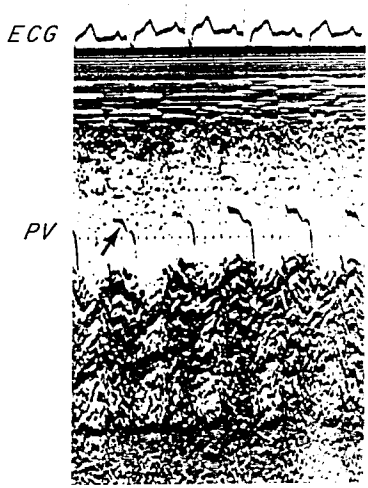

FIG. 13. Echocardiogram of the pulmonic valve (PV), demonstrating the characteristic pattern of motion of the posterior leaflet during late diastole. The arrow points to the pulmonic valve "a" wave, after which rapid posterior motion representing opening occurs. In mid-systole and early diastole, this echo disappears.

diminish some of the limitations of standard echocardiography. The most important applications of echocardiography are summarized in table 2.

Systolic Time Intervals, Phonocardiography and Apexcardiography

Definition of Systolic Time Intervals

Systolic time intervals are derived from the carotid pulse wave, phonocardiogram, and electrocardiogram. Figure 15 illustrates the derivation of some of these intervals: the duration of systole ($Q-A_2$), left ventricular ejection time (LVET), and the pre-ejection period (PEP). The left ventricular ejection time is the interval from the onset of the carotid pressure rise (O) to the dicrotic notch (DN) and is related to left ventricular stroke volume. Total electrical mechanical systole is the interval from the Q wave of the electrocardiogram to the aortic second sound ($Q-A_2$). Note that the dicrotic notch, reflecting aortic valve closure, follows the aortic second sound, A_2. This delay is due to the time required for pulse-wave transmission or the interval between aortic valve closure and the arrival of the dicrotic notch transmission wave at the external pressure transducer placed over the carotid artery. The difference between the $Q-A_2$ interval and the LVET is called the pre-ejection period (PEP). The PEP is composed of the isovolumic contraction time and the duration of electrical depolarization of the heart. Table 3 summarizes some of the important factors affecting the systolic time intervals.

Application to Left Ventricular Function

In the absence of aortic stenosis, the PEP and LVET have been used as indices of left ventricular function. The ratio PEP:LVET is used to increase the sensitivity of either interval used separately. For example, left ventricular dysfunction is usually characterized by an increase in PEP and a decrease in LVET or a marked increase in the PEP:LVET ratio. The systolic time intervals and the pulse-wave propagation time have been applied to the study of cardiac function during acute myocardial infarction, before and after cardiac surgery and in routine evaluation of cardiac outpatients suspected of having valvular lesions or left ventricular dysfunction. It should be understood that the PEP and LVET depend not only on left ventricular systolic function but also on left ventricular filling pressures and the status of the peripheral vasculature. Changes in the left ventricular preload and afterload may alter the systolic time intervals and obscure or mimic changes related to alterations in left ventricular function. During myocardial infarction, for example, changes in catecholamine level will lead to variable alterations in peripheral resistance. If arterial systolic pressure is increased in response to a high catecholamine output, PEP may increase but LVET, which is prolonged in response to increased afterload,

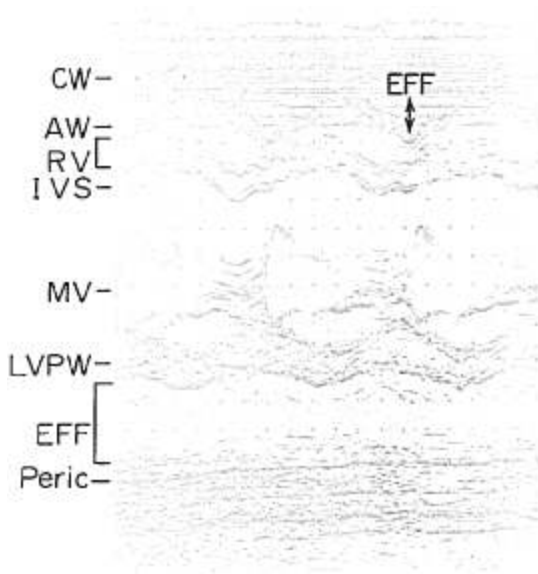

FIG. 14. Echocardiogram from a patient with anterior and posterior pericardial effusion (EFF). A space can be seen between the chest wall (CW) and the right ventricular anterior wall (AW) and between the left ventricular posterior wall (LVPW) and the pericardium (PERI). IVS = interventricular septum, MV = mitral valve, CW = chest wall.

TABLE 2. Some Important Applications of Echocardiography

I. Evaluation of left ventricular (LV) function
A. Estimation of ejection fraction from LV dimensions
B. Detection of abnormal LV wall motion and thickness (the posterior LV wall and intraventricular septum can be visualized best, the apex and anteriolateral wall less consistently)
C. Detection of altered mitral valve motion associated with LV dysfunction, *i.e.*, abnormal mitral valve closure in patients with elevated LV end-diastolic pressure and abnormal mitral valve diastolic configuration in patients with reduced LV compliance
D. Assessment of left atrial size
II. Evaluation of right ventricular (RV) function
A. Estimation of RV size from echocardiographic dimension
B. Detection of paradoxic motion of interventricular septum in patients with RV "volume overload" states
III. Diagnosis and quantification of pericardial effusion
IV. Analysis of valve function
A. Mitral valve: detection of characteristic changes in patients with mitral stenosis, IHSS, mitral valve prolapse, flail leaflet, left atrial myxoma, abnormal LV function
B. Tricuspid valve: similar to A above
C. Aortic valve: detection of thickening or calcification and detection of characteristic systolic "notch" in IHSS
D. Pulmonic valve: detection of pulmonary hypertension, diagnosis of pulmonic stenosis

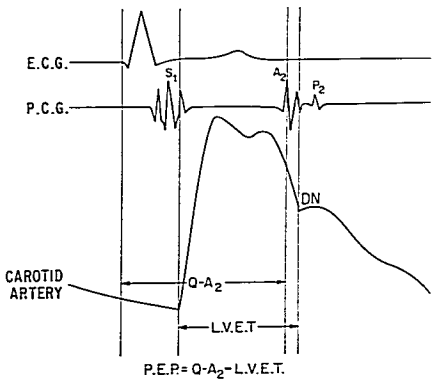

FIG. 15. Derivation of the systolic time intervals. PCG = phonocardiogram, DN = dicrotic notch, LVET = left ventricular ejection time, PEP = pre-ejection period, S_1 = first heart sound, A_2 = aortic component of second heart sound, P_2 = pulmonic component of second heart sound, Q = Q wave of ECG.

may increase even more. Thus, in some patients with left ventricular dysfunction, the expected increase in PEP:LVET may be obscured or attenuated in the presence of systolic hypertension related to high levels of circulating catecholamines. Patients undergoing general anesthesia may appear to have left ventricular dysfunction based on a high PEP:LVET ratio. However, this also reflects changes in left ventricular preload and afterload related to positive-pressure breathing and changes in systemic vascular resistance and venous capacitance.[30] A better analysis of left ventricular function may be provided by comparing measurements of the systolic time intervals obtained during two or more different physiologic states; for example, observation of changes in PEP and LVET during augmented venous return induced by passive leg raising or during diminution of afterload or preload following administration of nitroglycerin. A normally functioning left ventricle will tolerate augmented venous return without much change in its end-diastolic pressure, while a failing left ventricle may elevate its end-diastolic pressure, thus increasing PEP. In a normal heart, PEP will remain relatively fixed while LVET will increase secondary to an increasing stroke volume, thus shortening the PEP:LVET ratio. In the failing heart, PEP will increase along with the increase in LVET. Furthermore, if the stroke output of the failing heart is decreased, LVET will not increase appropriately, resulting in further prolongation of the PEP:LVET ratio. Since these intervals are related to so many variables, they must be interpreted with caution. Interpretation of these intervals may have more meaning in the light of additional information supplied by other noninvasive techniques such as echocardiography and radionuclide scanning.

Application to Aortic Stenosis

Systolic time intervals are also used in approximating the severity of aortic stenosis. A decrease in PEP and an increase in LVET or a substantial decrease in PEP:LVET ratio are observed in significant aortic stenosis. Other systolic time intervals are also useful in assessing the severity of aortic stenosis. These include: 1) the upstroke time (u time), or the interval between the onset of carotid pressure and peak pressure, and 2) the t time, or the time required for the pulse to attain half of its peak height. The rate of rise of the carotid pulse can be derived by dividing peripheral pulse pressure by the carotid upstroke time.

Phonocardiography

The phonocardiogram is most useful in analysis and timing of cardiac murmurs and

sounds. For example, a fourth heart sound plus first heart sound combination can be distinguished from a first heart sound plus early systolic click. The peak of the diamond-shaped systolic murmur of aortic stenosis occurs progressively later in systole with increasing aortic valve gradient. Thus, the Q wave-to-peak murmur interval can aid in the assessment of the severity of aortic stenosis. The opening snap of mitral stenosis moves progressively closer to the second sound as the mitral valve gradient increases. In pulmonic stenosis, the length of the murmur prolongs and the pulmonic ejection click occurs closer to the first heart sound with increasing severity. These indices are especially useful in following patients as their disease progresses.

An important application of the phonocardiogram has been the evaluation of prosthetic valve dysfunction associated with thrombosis or ball variance.[31]

Two additional techniques, apexcardiography (ACG) and kinetocardiography (KCG) are both based on the analysis of precordial motion imparted by left ventricular contraction and relaxation. The apexcardiogram is recorded by a pressure-sensitive transducer attached to the chest wall at the point of maximal impulse, while the kinetocardiogram is a recording from a similar transducer which is fixed to an external point.

Abnormalities of systolic and diastolic precordial motion usually reflect changes in preload and afterload. For example, both the apexcardiogram and the kinetocardiogram may show a long left ventricular systolic bulge or plateau in severe aortic stenosis and a double-peaked systolic wave in IHSS.

To a great extent the ACG and KCG and the phonocardiogram display visually what a clinician can palpate and auscult. However, timing of events in the cardiac cycle is more precise with these techniques and provides an objective monitoring of patients, especially those with valvular heart disease and with left ventricular dysfunction.

Radionuclide Imaging Techniques

Gamma radiation emitted from radioactive elements (radionuclides) is useful in noninvasive cardiac imaging for diagnosis and monitoring.[32,33] Radionuclide techniques involve intravenously injecting a radioisotopic tracer and producing a picture or image of its distribution.

Basic Principles

Two basic components are necessary for radionuclide monitoring: the radiopharmaceutical and the imaging device. The radiopharmaceutical is the substance injected into the patient. It contains the radionuclide, while the imaging device allows conversion of the invisible gamma rays emitted by the radio-

TABLE 3. Effects of Some Physiologic and Pharmacologic Interventions on Systolic Time Intervals

	LVET	PEP	PEP/LVET
I. Changes in afterload			
A. Increase (systemic hypertension, LV outflow obstruction), nitrous oxide	↑	↑	↑
B. Decrease (amyl nitrite vasodilators)	↓	⟷	↓
II. Changes in preload			
A. Increase (increased venous return, aortic regurgitation or mitral regurgitation)	↑	↓	↓
B. Decrease (decreased venous return, upright posture)	↓	↑	⟷
III. Changes in contractility			
A. Congestive heart failure	↓	↑	⟷
B. Hyperthyroidism	↓	↓	↓
C. Beta-adrenergic block (propranolol)	↑	↑	↑
D. Beta-adrenergic stimulation (isoproterenol)	↓	↓	↓
E. Anesthetic drugs (halothane, enflurane)	↓	↑	↑

nuclide into visible images that localize the radiopharmaceutical.

Radiopharmaceuticals

Four varieties of cardiac imaging are potentially useful in monitoring: 1) flow imaging and shunt detection, 2) cardiac blood pool imaging, 3) myocardial muscle imaging, and 4) myocardial infarct imaging. Technetium-99m is a radionuclide with gamma emissions especially suitable for imaging. It is used in many cardiac-imaging applications in various forms: 1) as a salt, technetium pertechnetate (TcO_4^-) for flow imaging; 2) electrolytically bound to serum albumin for blood pool studies; 3) bound to a phosphate or phosphonate complex that accumulates in myocardial infarction. Radionuclides that concentrate in normal myocardium have been used for myocardial (muscle) imaging. These include the monovalent cations potassium-43 ($^{43}K^+$), rubidium-81 ($^{81}Rb^+$) and cesium-129 ($^{129}Cs^+$). All of these agents are difficult to image due to their very high energy emissions, which are collected with low efficiency. Thallium-201 ($^{201}Tl^+$) has been recently introduced as a myocardial imaging material, and has lower energy emissions, which are more suitable for gamma camera imaging. The amount of radioactive nuclide is quantitated in terms of its radioactivity, which is expressed in curies, millicuries, or microcuries.

The Imaging Device

Gamma-ray emissions from the distribution of the "radiopharmaceutical" are converted into images by a rectilinear scanner or a gamma camera. The imaging system consists of three components: 1) the detector or camera, 2) the collimator, and 3) the display system. For the purpose of this review, the gamma camera, which is most frequently used for cardiac studies, is the only imaging device described. The second imaging device, the rectilinear scanner, has few applications in cardiac diagnosis or monitoring.

The gamma camera most commonly used is the Anger type. The Anger *camera* consists of a circular sodium iodide crystal (usually half an inch thick and 11 inches in diameter), a circular array of 19 or 37 photomultiplier tubes, and a lead housing. The sodium iodide crystal converts gamma rays into scintillations (or visible light). The nearest photomultiplier tubes sense and amplify the scintillation so that it can be displayed in perspective on an oscilloscope. The *collimator* is a circular sheet of lead with multiple holes (parallel, converging or diverging with respect to the center of the crystal), which fits over the scintillation crystal of the gamma camera. The collimator reduces the amount of scattered radiation that could degrade the final image. The *display system* usually consists of an oscilloscope and a Polaroid or celluloid film camera. A computer can be used to aid in image collection and to improve image contrast for easier definition of cardiac borders.

Flow Imaging and Shunt Detection

A bolus of technetium-99m pertechnetate injected intravenously into a peripheral vein can be imaged as it flows into the subclavian and innominate veins, superior vena cava, right-sided cardiac chambers, pulmonary arteries, lungs, and left-sided cardiac chambers (fig. 16). Polaroid or celluloid film images are taken in rapid succession, or the flow pattern is recorded on magnetic tape or a computer memory. These flow images can be used to identify chambers that may overlap in blood pool studies or to identify and quantitate intracardiac shunts.[34,35] For shunt detection, the camera is generally positioned to obtain an anteroposterior or left anterior oblique view to separate right- and left-sided chambers. A computer is used to derive time–activity curves that are proportional to flow through the cardiac chambers. Thus, when there is a right-to-left shunt, the curve will show early appearance of tracer within the left-sided chambers, whereas when there is a left-to-right shunt, a second peak of activity would be expected within the right side of the heart. Methodology for approximating shunt size is available.[35,36]

There are several clinical applications for this technique. Neonatal cyanosis may be due to pulmonary disease or to cardiac disease. A flow study could rule out significant right-to-left intracardiac shunting in the face of cyanotic pulmonary disease. Thus, the neonate with pulmonary cyanosis would avoid a

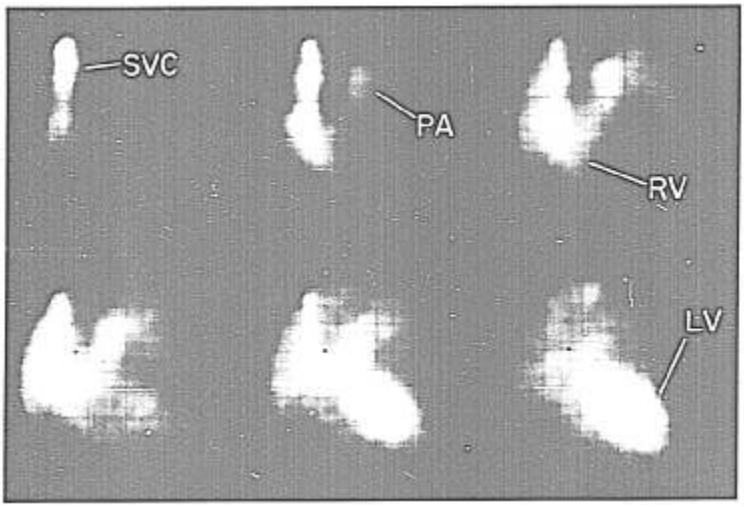

FIG. 16. Normal radionuclide flow study in the anteroposterior projection. A bolus of technetium-99m is followed on the gamma camera display as it passes from the right antecubital vein into the superior vena cava (SVC), right atrium and right ventricle (RV), pulmonary artery (PA), lungs, left atrium and left ventricle (LV). A computer can be used to generate time–activity curves. The region or chamber of interest is encircled and activity within that region is plotted. In the presence of a right-to-left shunt, activity would appear prematurely in the region of the LV, while in left-to-right shunts a second peak of activity would appear in the region of the pulmonary artery or lung.

potentially hazardous invasive angiographic study. Similarly, adults with possible intracardiac shunts can be studied to approximate the severity of the shunt.

Time–activity curves during the passage of radionuclide through the left ventricle have also been used to estimate ejection fraction.[37] This approach utilizes the counts contained in the peaks (end-diastole) and valleys (end-systole) of the left ventricular portion of the flow study with subtraction of the counts outside of the left ventricle (background) to compute ejection fraction. This technique is based upon the fact that there is little or no background activity in the blood on initial passage of radionuclide. Thus, only one or two studies are feasible before background activity precludes reliable determination of ejection fraction. Since the half life of technetium-99m is six hours, serial studies can be repeated only daily, thus limiting the application of this technique in monitoring.

GATED CARDIAC BLOOD POOL STUDIES

After equilibration of an intravenous injection of 15–20 millicuries of technetium-99m bound to human serum albumin (^{99m}Tc-HSA), an image obtained over the precordium demonstrates the cardiac blood pool. With appropriate positioning of the gamma camera, the heart can be studied in multiple projections. Synchronization of count collection with the electrocardiogram allows images to be obtained in end-systole (shortly after the peak of the T wave) and end-diastole (near the peak of the QRS complex).[38] Adequate images are obtained after two hundred thousand (200,000) counts or more have been collected. Approximately 5 to 10 minutes are required for each image. Counts are usually

collected for approximately an eighth of each cardiac cycle (between 500 and 100 msec) for end-systole and for end-diastole. A computer, magnetic tape recorder, or second oscilloscope allows simultaneous collection of systolic and diastolic images in 5–10 minutes. The resulting images represent an average of the end-systolic and end-diastolic volumes over the 5–10-minute imaging interval. The method for obtaining gated blood pool scan images is illustrated in figure 17. A 30 degree right anterior and 40–50-degree left anterior oblique view are routinely obtained, as illustrated in the normal study in figure 18. The gated cardiac blood pool scan has been useful in 1) evaluation of regional and global left ventricular performance,[38–42] evaluation of right ventricular function,[43] 3) observation of

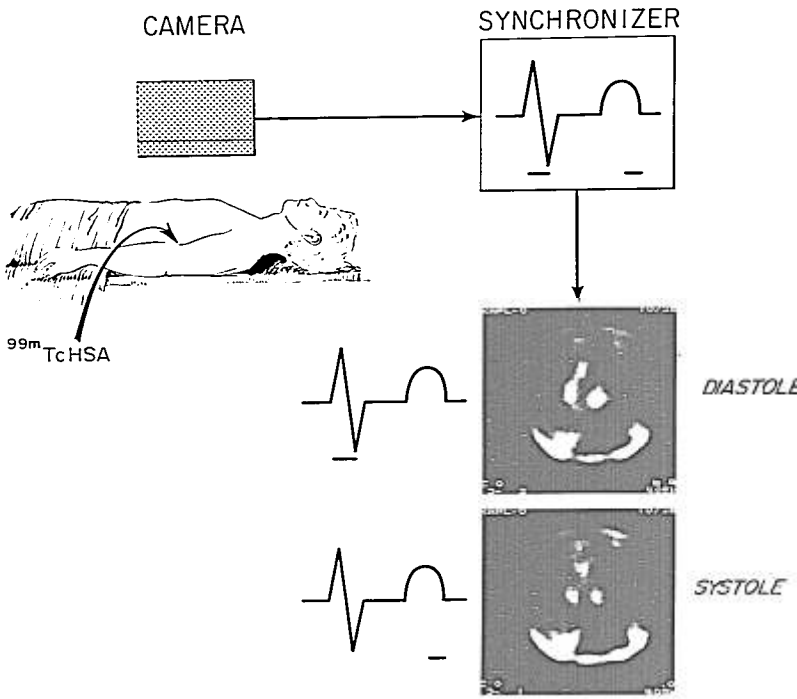

FIG. 17. Components necessary for obtaining the gated cardiac blood pool scan. Technetium-99m-tagged human serum albumin (^{99m}Tc-HSA) is given intravenously. The gamma *camera* collects counts producing an image of the cardiac blood pool. The *synchronizer* allows collection of counts to be gated by the electrocardiogram so that one image is collected during the QRS complex (end-*diastole*) and a second image during the latter portion of the T-wave (end-*systole*). The images displayed in this illustration were obtained in the 50-degree left anterior oblique projection.

The left ventricle (*right*) and right ventricle and pulmonary outflow tract (*left*) are easily identified. The interventricular septum is well defined, separating the two ventricles. Comparison of *diastole* and *systole* reveals normal concentric contraction of both ventricles.

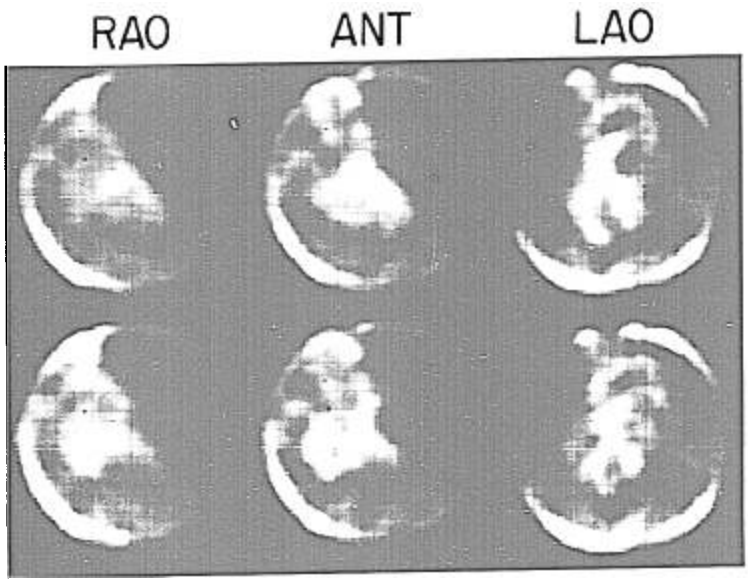

FIG. 18. Normal gated cardiac blood pool study in the 30-degree right anterior oblique (RAO), anteroposterior (ANT), and 50-degree left anterior oblique (LAO) projections. End-diastolic images are in the top row and end-systolic images in the bottom row. The left ventricular anterolateral, apical and inferior walls are demonstrated in the RAO and ANT projections. The right ventricle (*left*) is separated from the left ventricle (*right*) in the LAO projection. The pulmonary artery and aorta can be seen crossing one another in these LAO images.

interventricular septal configuration,[44,45] and 4) diagnosis of left atrial myxomas.[46,47]

Evaluation of Regional and Global Left Ventricular Function

Comparison of systolic and diastolic images allows evaluation of left ventricular wall motion. In the right anterior oblique projection, the anterolateral, apical and inferior left ventricular walls can be assessed, while in the left anterior oblique projection, the septal, infero-apical and posterior walls are observed. Figure 19 is an example of studies demonstrating abnormal regional wall motion. A left ventricular aneurysm is illustrated.

The end-diastolic volume of the left ventricle can be estimated by measurement of the major and minor dimensions (fig. 20). Since the parallel-hole collimator does not magnify, its diameter can be used as a reference to determine the left ventricular dimensions. Left ventricular ejection fraction (left ventricular stroke volume/left ventricular end-diastolic volume) can be determined using the modified method of Dodge[48] from the right and left anterior oblique images. The gated cardiac blood pool scan is potentially useful: 1) in monitoring of left ventricular function over an interval of as long as three hours after administration of technetium-99m albumin a) during myocardial infarction or b) during the postoperative period (*n.b.*, slow separation of technetium-99m from albumin gradually decreases the quality of the blood pool image since technetium leaves the

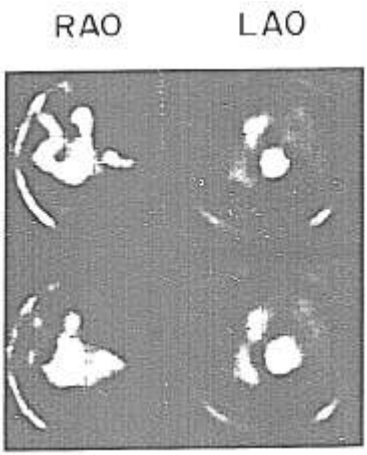

FIG. 19. Abnormal gated cardiac blood pool study in the 30-degree right anterior oblique (RAO) and 50-degree left anterior oblique (LAO) projections in a patient with a left ventricular aneurysm. Systolic images are in the top row and diastolic images in the bottom row. The RAO demonstrates a left ventricular aneurysm involving the anterolateral and apical segments.

blood pool to enter the interstitial and intercellular spaces. Since the physical half-life of technetium-99m is six hours, an interval of 12 hours or more must elapse before another dose of ^{99m}Tc-albumin will produce useful images. In the future other blood pool agents may be more stable); 2) for serial evaluation of left ventricular function in patients with valvular heart disease once or twice a year to help decide when surgery is indicated (*e.g.*, perhaps when ejection fraction begins to deteriorate) (figs. 21 and 22); 3) to assess ventricular function before major surgery; 4) to differentiate between operable (discrete left ventricular aneurysm) and inoperable (diffuse left ventricular dysfunction) causes of congestive heart failure that develops after myocardial infarction.

Evaluation of Right Ventricular Function

In an appropriate left anterior oblique position (30–60 degrees), the right ventricle (RV) can be separated from the left ventricle (LV)

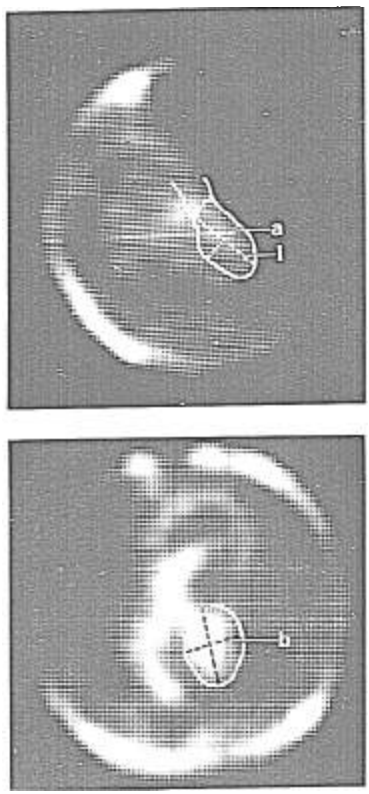

FIG. 20*A* (*above*), 30-degree right anterior oblique (RAO) and *B* (*below*), 50-degree left anterior oblique (LAO) end diastolic images, demonstrating the outline of the left ventricle and the axes used in estimation of its volume by the Dodge technique. The long major axis (l), and two minor axes (a) in the RAO and (b) in LAO are used to compute the volume:

$$\frac{4}{3}\pi\frac{a}{2}\frac{b}{2}\frac{l}{2} = \frac{ab\pi}{6}\,l = \text{LV volume}$$

The ejection fraction is determined by computing end-diastolic (ED) and end-systolic (ES) volumes as follows:

$$EF = \frac{ED - ES}{ED}$$

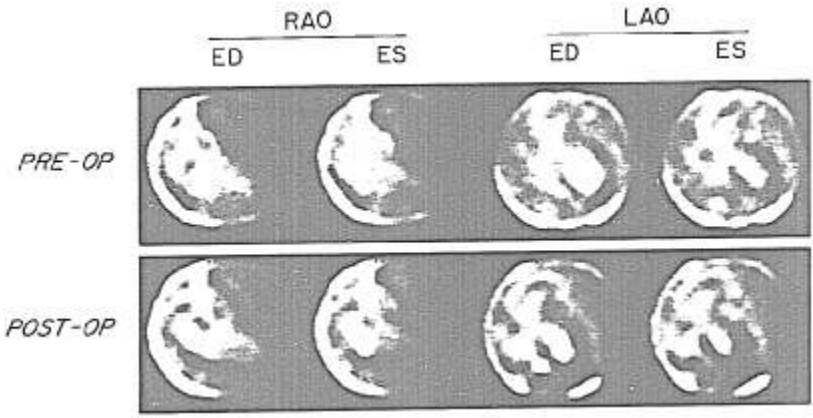

FIG. 21. Pre- and postoperative gated cardiac blood pool scans on a patient with mixed aortic valve disease (*i.e.*, regurgitation and stenosis) and normal coronary arteries who underwent aortic-valve replacement. The right anterior oblique (RAO) and left anterior oblique (LAO) images demonstrate normal left ventricular PRE-OP ejection fraction and contraction pattern. The left ventricular end-diastolic volume is increased (best defined in the LAO projection). POST-OP, the end-diastolic (ED) and end-systolic (ES) left ventricular volumes have decreased significantly. While the ejection fraction continues to be within normal range, the interventricular septum as observed in the LAO projection demonstrates reduced or absent excursion, a finding that appears to occur frequently after aortic-valve replacement.

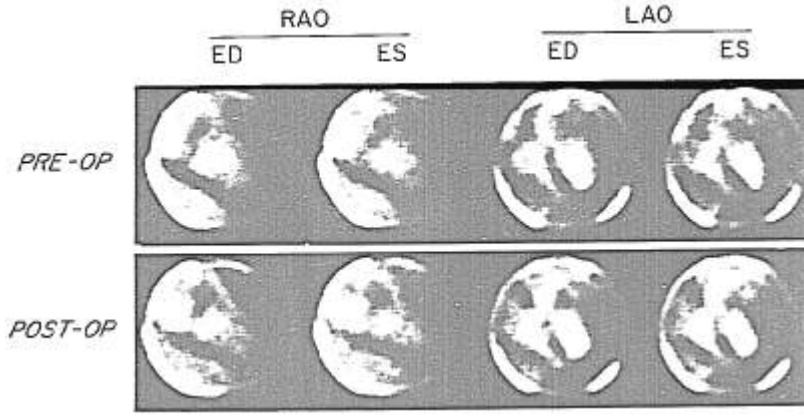

FIG. 22. Pre- and postoperative gated cardiac blood pool scans on a second patient with mixed aortic valve disease and normal coronary arteries who underwent aortic valve replacement. The preoperative right anterior oblique (RAO) and left anterior oblique (LAO) images demonstrate an end-diastolic (ED) volume comparable to that of the patient in figure 21. The ejection fraction, however, is remarkably diminished. POST-OP, the left ventricular ED volume as decreased somewhat; however, the ejection fraction has not improved. The decreased excursion of the interventricular septum is again evident in the postoperative LAO images (ES = end-systole).

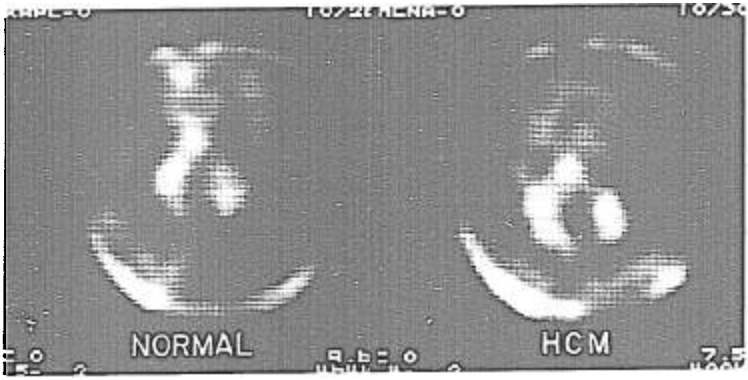

FIG. 23. End-diastolic gated cardiac blood pool images, demonstrating the configurations of the interventricular septum in a *normal* person and in a patient with hypertrophic cardiomyopathy (HCM) in a left anterior oblique projection. The normal septum is curvilinear with its concavity facing the left ventricle (*right*). The septum in HCM is straightened and frequently shows disproportionate upper septal thickening. Other characteristics of HCM are systolic cavity obliteration and a circular defect in the region of the left ventricular outflow tract produced by the bulky interventricular septum displacing blood pool activity. The latter are observed in the right anterior oblique image.

(fig. 20*B*). The size of the right ventricle can be estimated by measurement of its width during end-diastole. The RV is normally substantially narrower than the LV. Comparison of systolic and diastolic images demonstrates qualitatively the contractile ability of the RV. Thus, RV function can be monitored during a three-hour interval after a single dose of ^{99m}Tc-albumin or sequentially every 12 hours using repeated doses of ^{99m}Tc-albumin.

Examination of the RV in patients with atrial septal defect or other anomalies associated with large left-to-right shunts demonstrates a large end-diastolic volume with vigorous emptying. In patients with RV infarction, the chamber is enlarged, but has poor contractile function.[43] The complex geometry of the RV does not allow a simple model to be used to derive its volume or ejection fraction. The gated scan, however, may allow us to measure changes in function in a particular patient and following a particular therapeutic modality.

Observation of Intraventricular Septal Configuration

Since the left and right ventricles are seen on gated blood pool images, appropriate positioning of the gamma camera allows maximal separation of the two ventricles and observation of the interventricular septum. In order to study the configuration of the interventricular septum and the distribution of septal muscle, one must attempt to obtain an image in which the septum appears to be of uniform thickness from top to bottom. A diagnosis of hypertrophic cardiomyopathy ("idiopathic hypertrophic subaortic stenosis' [IHSS] when there is obstruction of LV outflow) may be suggested by an abnormal configuration of the interventricular septum. Normally in diastole the septum is concave towards the LV and is uniform in thickness from top to bottom. In hypertrophic cardiomyopathy, the septum usually appears thickened and flattened (*i.e.*, with loss of normal LV concavity). Frequently, in the diastolic image, the upper septum is disproportionately thickened in a suitable oblique view (fig. 23).[45] Right ventricular volume and pressure overload also tend to straighten the interventricular septum. Associated right ventricular enlargement can also be identified on the gated diastolic image and associated septal flattening should not be confused with that due to hypertrophic cardiomyopathy. Usually, the septum retains its normal configuration in hypertrophy secondary to hypertension or valvular aortic stenosis and

may appear normal or thickened. Monitoring configuration of the interventricular septum may provide insight into acute changes in right or left ventricular preload or afterload. For example, if the right ventricular systolic pressure increases abruptly, the interventricular septum may lose its curvature and, like a pressure transducer, reflect the difference in pressure between the two chambers.

Diagnosis of Atrial Myxoma

On the gated blood pool scan atrial myxomas can be seen as filling defects that occupy the left ventricle in diastole and the left atrium in systole.[46,47] Occasionally, a multilobulated myxoma remains unseen due to the small size of the lobules.

Myocardial Imaging

Ionic potassium and analogous cationic substances concentrate in myocardial cells through active transport (via the sodium–potassium–ATPase system located in the cell membrane). Intravenous administration of certain radionuclides of these cations may be employed in producing images of the myocardium using a gamma camera. Potassium-43,[49] rubidium-81,[50] cesium-129,[51] and (most recently) thallium-201 are the radionuclides most commonly used because the energy of these is most suitable for imaging with the gamma camera. The gamma emissions of ^{43}K, ^{81}Rb, and ^{129}Cs are too high to produce adequate images without a specialized collimator to diminish scatter and improve image quality. Thallium-201 emissions are of lower energy and easily imaged with a gamma camera equipped with a standard collimator.[52,53]

Normal myocardial images show a rela-

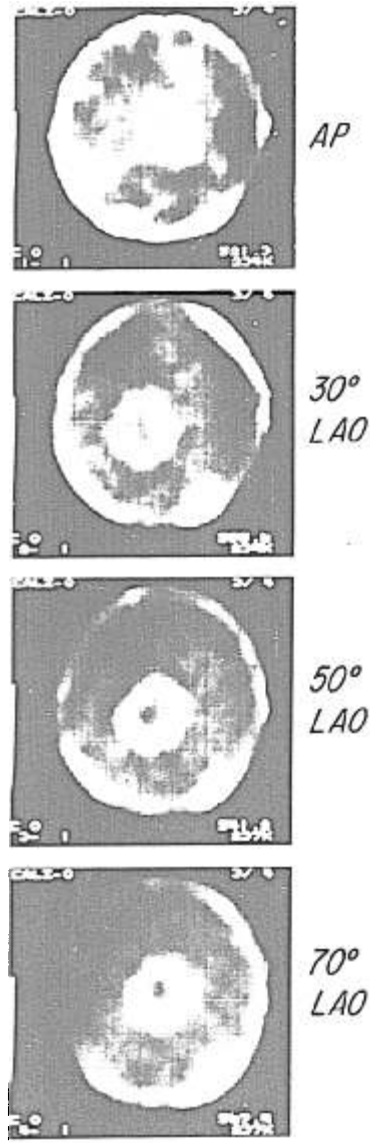

FIG. 24. Normal myocardial images obtained after intravenous injection of thallium-201. Only the left ventricle is observed. In the anteroposterior (AP) projection, the left ventricle apex points downward and to the right side of the picture. The inflow tract of the left ventricle (mitral-valve region, *left*) does not show activity and thus gives the AP view a "U"-shaped configuration. The remaining images in the left anterior oblique (LAO) projection have a "doughnut" appearance with the septum on the left and posterior wall on the right aspect of the image. Note that activity is homogeneously distributed. The left ventricular blood pool is located within the boundaries of the myocardial image and appears as a dark region without significant activity.

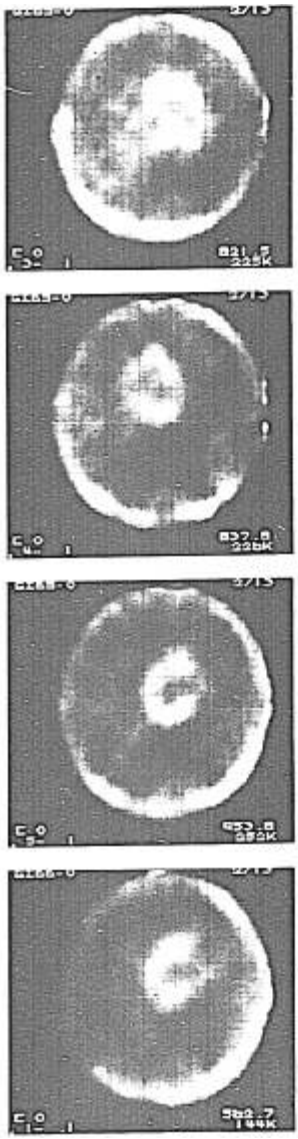

tively homogeneous distribution of these radionuclides throughout the left ventricle (fig. 24). In the anteroposterior view, the apical, inferior and lateral walls of the left ventricle can be examined. Multiple left anterior oblique views provide images of the septum, apical inferior and posterior left ventricular walls. Thallium-201 is presently the agent that produces the best images with a standard gamma camera. Thus, the myocardial images illustrated have been obtained employing this agent. Thallium is practically completely extracted from the blood by the myocardium as it passes through the coronary circulation, which means that images obtained early after intravenous administration depict perfusion pattern. After an intravenous dose of ^{201} Tl, background activity contained within the blood pool remains significant for 10–30 minutes, after which time imaging can commence. One to two millicuries of thallium-201 are usually given. Hepatic uptake is evident and is especially prominent in the postabsorptive period. The inferior wall may be obscured by hepatic activity, and thus thallium imaging is optimally accomplished in the fasting patient.

Acute or old myocardial damage appears as a region of diminished or absent activity (fig. 25) or a "cold spot." Cold regions or defects not present at rest can be induced by exercise. These defects appear to represent reversible ischemia and may be helpful in estimating the quantity of myocardium jeopardized by coronary-artery occlusive disease. The radionuclide stress test is reported to improve the sensitivity of the exercise electrocardiogram alone[54] in identifying patients with significant coronary-artery stenosis. A study at rest is necessary to determine whether a given cold spot is scar or transient exercise-induced ischemia. If delayed images are obtained over a four-to-six-hour interval after a defect has been observed on a post-exercise image, defects due to ischemia disappear, while defects due to scar persist. Serial myocardial scanning after a single intravenous

FIG. 25. Abnormal thallium-201 myocardial images, demonstrating a region of decreased or absent activity in the posterolateral wall consistent with a previous posterior wall myocardial infarction. The defect is best defined in the 50-degree and 70-degree left anterior oblique (LAO) projections, and appears as a disruption in the normally circular distribution of activity.

dose of thallium-201 may provide a means of differentiating between transient ischemia and persistent damage.[55]

Serial imaging after a single dose of ^{201}Tl may be useful in monitoring the critically ill patient in and out of the operating room. For example, the possibility of myocardial damage may be questioned in the case of a patient who has sustained a period of hypotension. A myocardial image 30 minutes after ^{201}Tl administration will delineate the perfusion pattern. Regions of the heart receiving adequate blood flow will take up activity maximally, while areas receiving inadequate blood flow will show diminished activity. The size of the region of diminished activity will be related to the quantity of muscle jeopardized or damaged by the coronary-artery disease. "Cold regions" on initial thallium images that fill in during a series of images have probably undergone a beneficial change in regional blood flow or in ability of that region to extract thallium (*e.g.*, due to reversal of ischemia), whereas "cold regions" that persist probably represent myocardial infarction.

Myocardial Infarction Imaging

Myocardial imaging allows delineation of myocardial infarction by demonstrating a region of diminished or absent activity. However, it does not allow differentiation of recent and old myocardial infarction. Other techniques for evaluation of myocardial infarction such as electrocardiography and serum enzyme analysis provide only indirect information about its presence, location and size.

Radiopharmaceuticals that concentrate in acutely infarcted myocardium to produce a "hot spot" image include ^{203}Hg-labeled chlormerodrin, ^{99m}Tc-labeled tetracycline,[56] and ^{99m}Tc-labeled pyrophosphate. The latter and its analogs appear to be the most useful.[57,58]

Technetium-99m-labeled sodium pyrophosphate is usually employed in bone imaging. During myocardial infarction, this phosphate compound probably combines with mitochondrial calcium, since complexes of calcium phosphate (hydroxyapatite) are known to precipitate during myocardial infarction.[59] Forty-five minutes to an hour after administration, Tc^{99m}-pyrophosphate can be imaged in recently infarcted myocardium. Uptake of pyrophosphate does not appear to be adequate for imaging until 12 hours or more after the onset of infarction. If the infarct is transmural, a localized region of pyrophosphate uptake can usually be defined. A more diffuse type of uptake is usually observed in subendocardial infarction. "Hot spots" can be obscured by osseous activity in the region of the heart (ribs, sternum, vertebrae); however, multiple views and computer programs to subtract rib activity have been employed to improve infarct detection.

Potential Applications of Radionuclide Imaging of the Heart

The radionuclide techniques described above, *i.e.*, flow, gated blood pool, myocardial and myocardial infarction imaging, are newcomers to the field of noninvasive cardiology. Aside from their potential as diagnostic tests (see table 1), they may provide a means for assessing the heart before and after cardiac as well as noncardiac surgery. In the elderly patient who is about to undergo major elective or semielective surgery (*e.g.*, repair of an abdominal aortic aneurysm), the gated blood pool scan can be used to determine left ventricular ejection fraction, an important indicator of left ventricular function. Intraoperative myocardial infarction can be detected by postoperative myocardial scanning with thallium-201 (to demonstrate a "cold spot") and technetium-99m pyrophosphate (to demonstrate a "hot spot") at a time when serum enzymes are not a reliable indicator of infarction. The efficacy of coronary-artery-bypass surgery might be assessed by pre- and postoperative myocardial scanning after exercise. Comparison of ejection fraction and ventricular volumes before and after valve replacement would allow us to study the beneficial effects of the operation and to determine prognosis (figs. 21 and 22). "Portable" gamma cameras that can be moved to the patients' bedsides are already in use in coronary care units for evaluating patients admitted with ischemic cardiac symptoms. In the future, these cameras may play a role in the cardiac assessment of patients after surgical procedures in surgical intensive care units.

Many of the echocardiograms were generously provided by Dr. Gordon S. Myers for the Noninvasive Diagnostic Laboratory of the Massachusetts General Hospital.

Background Reading

a. Feigenbaum H: Echocardiography. Philadelphia, Lea and Febiger, 1972
b. Tavel ME: Clinical Phonocardiography and External Pulse Recording. Chicago, Yearbook Medical Publishers, 1972
c. Weissler AM: Noninvasive Cardiology. New York, Grune and Stratton, 1974
d. Strauss HW, Pitt B, James AE: Cardiovascular Nuclear Medicine. St. Louis, C.V. Mosby, 1974

References

1. Troy BL, Pombo JF, Rackley CF: Measurement of left ventricular wall thickness and mass by echocardiography. Circulation 45:602–611, 1972
2. Feigenbaum H, Popp RL, Chip JN, et al: Left ventricular wall thickness measured by ultrasound. Arch Intern Med 121:391–395, 1968
3. Henry WL, Clark CE, Epstein SE: Asymmetric septal hypertrophy. Echocardiographic identification of the pathognomonic anatomic abnormality of IHSS. Circulation 47:225–233, 1973
4. Feigenbaum H, Popp RL, Wolfe SB, et al: Ultrasound measurements of the left ventricle: A correlative study with angiocardiography. Arch Intern Med 129:461–467, 1972
5. Pombo JF, Troy BL, Russell RO Jr: Left ventricular volumes and ejection fraction by echocardiography. Circulation 43:480–490, 1971
6. Ludbrook P, Karliner JS, Peterson K, et al: Comparison of ultrasound and cineangiographic measurements of left ventricular performance in patients with and without wall motion abnormalities. Br Heart J 35: 1026–1032, 1973
7. Teichholz LE, Kreulen T, Herman MV, et al: Problems in echocardiographic volume determinations: Echocardiographic–angiographic correlations in the presence or absence of asynergy. Am J Cardiol 37: 7–11, 1976
8. Fortuin NJ, Hood WP Jr, Craige E: Evaluation of left ventricular function by echocardiography. Circulation 46:26–35, 1972
9. Corya BC, Rasmussen S, Knoebel SB, et al: Echocardiography in acute myocardial infarction. Am J Cardiol 36:1–10, 1975
10. Hagan AD, Francis GS, Sahn DJ, et al: Ultrasound evaluation of systolic anterior septal motion in patients with and without right ventricular volume overload. Circulation 50: 248–254, 1974
11. DeMaria AN, Miller RR, Amsterdam EA, et al: Mitral valve early diastolic closing velocity in the echocardiogram. Relation to sequential diastolic flow and ventricular compliance. Am J Cardiol 37:693–700, 1976
12. Gustafson A: Correlation between ultrasound cardiography, hemodynamics and surgical findings in mitral stenosis. Am J Cardiol 19:32–41, 1967
13. Duchak JM Jr, Chang S, Feigenbaum H: The posterior mitral valve echo and the echocardiographic diagnosis of mitral stenosis. Am J Cardiol 29:628–632, 1972
14. DeMaria AN, King JF, Bugren HG, et al: The variable spectrum of echocardiographic manifestations of the mitral valve prolapse syndrome. Circulation 50:33–41, 1974
15. Jeresaty RM, Landry AB, Liss JP: "Silent" mitral valve prolapse. Analysis of thirty-two cases. Am J Cardiol 35:146, 1975
16. Popp RL, Harrison DC: Ultrasound in the diagnosis and evaluation of therapy of idiopathic hypertrophic subaortic stenosis. Circulation 40:905–914, 1969
17. Henry WL, Clark CE, Griffith JM, et al: Mechanism of left ventricular outflow obstruction in patients with obstructive asymmetric septal hypertrophy (idiopathic hypertrophic subaortic stenosis). Am J Cardiol 35:337–345, 1975
18. DeMaria AN, King DK, Salel AF, et al: Echocardiography and phonocardiography of acute aortic regurgitation in bacterial endocarditis. Ann Intern Med 82:329–335, 1975
19. Konecke LL, Feigenbaum H, Chang S: Abnormal mitral valve motion in patients with elevated left ventricular diastolic pressures. Circulation 47:989–996, 1973
20. Hirata T, Wolfe SB, Popp RL, et al: Estimation of left atrial size using ultrasound. Am Heart J 78:43–52, 1969
21. Brown OR, Harrison DC, Popp RL: An improved method for echocardiographic detection of left atrial enlargement. Circulation 50:58–64, 1974
22. Nasser WK, Davis RH, Dillon JC, et al: Atrial myxoma, II. Phonocardiographic, echocardiographic, hemodynamic and angiographic features in nine cases. Am Heart J 83:810–824, 1972
23. Feizi O, Symons C, Yacoub M: Echocardiography of the aortic valve. Br Heart J 36: 341–351, 1974
24. Weyman AE, Feigenbaum H, Dillon JC, et al: Cross-sectional echocardiography in assessing the severity of valvular aortic stenosis. Circulation 52:828–834, 1975
25. Weyman AE, Dillon JC, Feigenbaum H, et al: Echocardiographic patterns of pulmonic valve motion with pulmonary hypertension. Circulation 50:905–910, 1974
26. Weyman AE, Dillon JC, Feigenbaum H, et al: Echocardiographic patterns of pulmonary valve motion in valvular pulmonic stenosis. Am J Cardiol 34:644–651, 1974
27. Horowitz MS, Schultz CS, Stinson EB, et al: Sensitivity and specificity of echocardiographic diagnosis of pericardial effusion. Circulation 50:239–247, 1974
28. Williams RS, Tucker CR: Echocardiographic Diagnosis of Congenital Heart Disease. Boston, Little, Brown and Co., 1976 (in press)
29. Solinger R, Elbl F, Minhas K: Deductive

echocardiographic analysis in infants with congenital heart disease. Circulation 50: 1072–1096, 1974
30. Dauchot PJ, Rasmussen JP, Nicholson DH: On-line systolic time intervals during anesthesia in patients with and without heart disease. ANESTHESIOLOGY 44:472–480, 1976
31. Hylen JC: Mechanical malfunction and thrombosis of prosthetic heart valves. Am J Cardiol 30:396–404, 1972
32. Strauss HW, Pitt B, James AE: Cardiovascular Nuclear Medicine. St. Louis, C. V. Mosby, 1974
33. Wagner HN Jr: Nuclear medicine in cardiovascular disease. Hosp Prac 7:108–116, 1972
34. Gates GF, Orme HW, Dore EK: Cardiac surgery in cyanotic children assessed by ^{99m}Tc-microaggregated albumin (MAA). J Nucl Med 14:398, 1973
35. Maltz DL, Treves S: Quantification of left-to-right shunts by radionuclide angiocardiography in children. J Nucl Med 13:787–788, 1972
36. Strauss HW: Detection and quantification of intracardiac shunts. Cardiovascular Nuclear Medicine. Edited by HW Strauss, B Pitt, AE James. St. Louis, C.V. Mosby, 1974
37. Ashburn WL, Kostuk WJ, Karliner JS, et al: Left ventricular volume and ejection fraction determination by radionuclide angiography. Semin Nucl Med 3:165–176, 1973
38. Strauss HW, Zaret BL, Hurley PJ, et al: A scintiphotographic method for measuring left ventricular ejection fraction in man without cardiac catheterization. Am J Cardiol 28:575–580, 1971
39. Zaret BL, Strauss HW, Hurley PJ, et al: A noninvasive scintiphotographic method for detecting regional ventricular dysfunction in man. N Engl J Med 284:1165–1170, 1971
40. Rigo P, Murray M, Strauss HW, et al: Left ventricular function in acute myocardial infarction evaluated by gated scintiphotography. Circulation 50:678–684, 1974
41. Rigo P, Murray M, Strauss HW, et al: Scintiphotographic evaluation of patients with suspected left ventricular aneurysm. Circulation 50:985–991, 1974
42. Schulze RA Jr, Rouleau J, Rigo P, et al: Ventricular arrhythmias in the late hospital phase of acute myocardial infarction: Relation to left ventricular function detected by gated cardiac blood pool scanning. Circulation 52:1006–1011, 1975
43. Rigo P, Murray M, Taylor R, et al: Right ventricular dysfunction detected by gated scintiphotography in patients with acute inferior myocardial infarction. Circulation 52: 268–274, 1975
44. Bulkley BH, Rouleau J, Strauss HW, et al: Idiopathic hypertrophic subaortic stenosis: Detection by thallium 201 myocardial perfusion imaging. N Engl J Med 293:1113–1116, 1975
45. Pohost G, Dinsmore R, Block P, et al: ASH or DUST? Circulation 52:suppl II (abstr.) 140, 1975
46. Zaret BL, Hurley PJ, Pitt B: Noninvasive scintiphotographic diagnosis of left atrial myxoma. J Nucl Med 13:81–84, 1972
47. Pohost GM, Dinsmore RE, McKusick KA, et al: Improved detection of left atrial myxoma by computerized gated radionuclide scanning. Clin Res (abstr) 23:202A, 1975
48. Dodge HT, Sandler H, Ballew DH, et al: Use of biplane angiography for the measurement of left ventricular volume in man. Am Heart J 60:762–776, 1960
49. Botti RE, MacIntyre WJ, Pritchard WH: Identification of ischemia area of left ventricle by visualization of ^{42}K myocardial deposition. Circulation 47:486–492, 1973
50. Martin ND, Zaret BL, McGowan RL, et al: Rubidium-81: A new myocardial scanning agent: Noninvasive regional myocardial perfusion scans at rest and exercise and comparison with potassium-43. Radiology 111:651–656, 1974
51. Ronhilt DW, Adolph RJ, Sodd VJ, et al: Cesium-129 myocardial scintigraphy to detect myocardial infarction. Circulation 48:1242–1251, 1973
52. Bradley-Moore PR, Lebowitz E, Greene MW, et al: Thallium-201 for medical use. II: Biologic behavior. J Nucl Med 16:156–160, 1975
53. Strauss HW, Harrison K, Langan JK, et al: Thallium-201 for myocardial imaging: Relation of thallium-201 to regional myocardial perfusion. Circulation 51(4):641–645, 1975
54. Zaret BL, Stenson RE, Martin ND, et al: Potassium-43 myocardial perfusion scanning for the noninvasive evaluation of patients with false-positive exercise tests. Circulation 48:1234–1241, 1973
55. Pohost GM, Beller GA, Moore RH, et al: Redistribution of thallium-201 following transient myocardial ischemia. Clin Res (abstr) 24:235A, 1976
56. Holman BL, Lesch M, Zweiman FG, et al: Detection and sizing of acute myocardial infarcts with ^{99m}Tc (SN) tetracycline. N Engl J Med 291:159–163, 1974
57. Parkey RW, Bonte FJ, Meyer SL, et al: A new method for radionuclide imaging of acute myocardial infarction in humans. Circulation 50:540–546, 1974
58. Willerson JT, Parkey RW, Bonte FJ, et al: Acute subendocardial myocardial infarction in patients. Its detection by technetium 99m stannous pyrophosphate myocardial scintigrams. Circulation 51:436–441, 1975
59. D'Agostino AN, Chiga M: Mitochondrial mineralization in human myocardium. Am J Clin Pathol 53:820–824, 1970